

Increased huntingtin protein length reduces the number of polyglutamine-induced gene expression changes in mouse models of Huntington's disease

Edmond Y.W. Chan^{1,†}, Ruth Luthi-Carter^{2,†}, Andrew Strand³, Steven M. Solano², Sarah A. Hanson², Molly M. DeJohn², Charles Kooperberg³, Kathryn O. Chase⁴, Marian DiFiglia⁵, Anne B. Young², Blair R. Leavitt¹, Jang-Ho J. Cha², Neil Aronin⁴, Michael R. Hayden¹ and James M. Olson^{3,*}

¹Center for Molecular Medicine and Therapeutics, Department of Medical Genetics, Children's and Women's Hospital, University of British Columbia, Vancouver, British Columbia, Canada, V5H 4H4, ²Center for Aging, Genetics and Neurodegeneration, Massachusetts General Hospital, Charlestown, MA 02129-4404, USA, ³Fred Hutchinson Cancer Research Center, Seattle, WA 98195, USA, ⁴Department of Medicine, University of Massachusetts Medical School, Worcester, MA 01655, USA and ⁵Department of Neurology, Massachusetts General Hospital, Boston, MA 02114, USA

Received March 12, 2002; Revised and Accepted June 7, 2002

Both transcriptional dysregulation and proteolysis of mutant huntingtin (htt) are postulated to be important components of Huntington's disease (HD) pathogenesis. In previous studies, we demonstrated that transgenic mice that express short mutant htt fragments containing 171 or fewer N-terminal residues (R6/2 and N171-82Q mice) recapitulate many of the mRNA changes observed in human HD brain. To examine whether htt protein length influences the ability of its expanded polyglutamine domain to alter gene expression, we conducted mRNA profiling analyses of mice that express an extended N-terminal fragment (HD46, HD100; 964 amino acids) or full-length (YAC72; 3144 amino acids) mutant htt transprotein. Oligonucleotide microarray analyses of HD46 and YAC72 mice identified fewer differentially expressed mRNAs than were seen in transgenic mice expressing short N-terminal mutant htt fragments. Histologic analyses also detected limited changes in these mice (small decreases in adenosine A2a receptor mRNA and dopamine D2 receptor binding in HD100 animals; small increases in dopamine D1 receptor binding in HD46 and HD100 mice). Neither HD46 nor YAC72 mice exhibited altered mRNA levels similar to those observed previously in R6/2 mice, N171-82Q mice or human HD patients. These findings suggest that htt protein length influences the ability of an expanded polyglutamine domain to alter gene expression. Furthermore, our findings suggest that short N-terminal fragments of mutant htt might be responsible for the gene expression alterations observed in human HD brain.

INTRODUCTION

The Huntington's disease (HD) gene (*IT15*) encodes a 3144-amino-acid protein of unknown function (huntingtin, htt). In HD, expansion of the polyglutamine [poly(Q)] tract, which begins 18 amino acid residues from the N terminus, leads to cellular dysfunction and neuronal death (1). Neurodegeneration in HD is cell-type-specific and medium spiny neurons of the striatum are most severely vulnerable (2–4). Much evidence supports the hypothesis that proteolysis of htt is an important step in HD pathogenesis (5–9), including the detection of htt

fragments in HD patient brains (10–13). htt can be cleaved into N-terminal fragments by caspases at particular sites, and caspase cleavage products may be hydrolyzed further by calpains and the 26S proteasome (12–16). In HD brain tissues, both wild-type and expanded forms of htt are proteolytically processed (11–13). Since caspase-cleaved wild-type htt fragments are also detectable in control brain tissues, proteolysis could be a normal part of htt function or turnover (12,13,17). In addition, caspase-cleaved htt has been observed in brain tissues from the YAC72 HD mouse model before onset of neurodegeneration (13).

*To whom correspondence should be addressed at: Fred Hutchinson Cancer Research Center, D4-100, 1100 Fairview Ave N, Seattle, WA 98109, USA. Tel: +1 2066677955; Fax: +1 2066672917; Email: jolson@fhcrc.org

[†]The authors wish it be known that, in their opinion the first two authors should be regarded as joint First Authors.

Cleavage of mutant htt is hypothesized to enhance the toxicity of its expanded poly(Q) tract. In support of this theory, shorter N-terminal fragments of mutant htt have the greatest effects on cell viability in cell culture systems (6,18), and generally produce the most severe phenotypes in transgenic mice (19,20). Full-length htt is mostly cytosolic, but short N-terminal fragments of mutant htt appear to become concentrated over time in neuronal nuclei (6,21–25). Recently, full-length htt or N-terminal htt fragments have been shown to interact with transcriptional regulators such as N-CoR, p53, cAMP response element-binding protein (CREB)-binding protein (CBP), mSin3a, CA150, p300, p300/CBP-associated factor (P/CAF), C-terminal-binding protein transcriptional co-repressor (CtBP), TAFII130 and Sp1 (26–33). These proteins can affect transcription directly as transactivators (or repressors) or indirectly through histone acetylation. Thus, proteolytic processing of htt could promote the entry of short poly(Q)-containing htt fragments into the nucleus, where they could more readily interact with transcriptional regulators and perturb gene expression.

Alterations in gene expression have been investigated to gain insight into the pathogenic mechanisms of HD. Decreased levels of neurotransmitter receptor and preproenkephalin mRNAs have been observed in HD patient postmortem striatal tissues, with neuropathology ranging from grade 0 (no macroscopic atrophy) to grade 3 (significant atrophy) (34,35). Also, decreases in dopamine receptors can be observed *in vivo* by positron emission tomography early in the disease process (36). Some of the mRNA alterations seen in human HD brain are recapitulated in R6/2 transgenic mice that express a short exon 1-encoded N-terminal fragment of htt (37–39). N-terminal fragments of htt can also produce gene expression

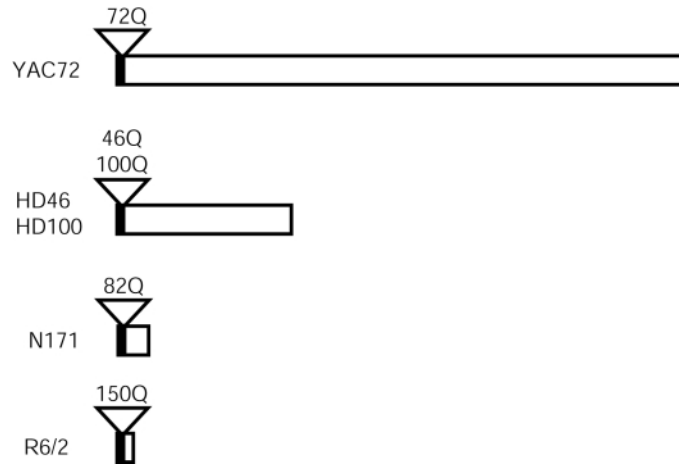


Figure 1. Schematic diagram illustrating relative sizes of huntingtin transproteins in YAC72, HD46, HD100, N171 and R6/2 transgenic mice. Huntingtin (htt) proteins represented to scale. In YAC72 line 2511, the full-length human htt transprotein (3144 amino acids) is coded by the complete human *IT15* gene containing 72 CAG repeats. In YAC72 mice, expression is driven by the *IT15* promoter. In transgenic lines HD46 and HD100, 964 amino acid residues of the htt N terminus, containing 46 or 100 CAG repeats, respectively, are expressed from the 5' one-third of the *IT15* cDNA under control of the *neuron-specific enolase* promoter. For comparison, we used data gathered in N171 transgenic mice that express, under control of the *prion* promoter, a short N-terminal fragment of htt (residues 1–171) containing 82 glutamine (Q) residues (23,44). N171-82Q mice were analyzed at a late symptomatic stage (4 months of age), at which these animals exhibit cytoplasmic neuronal inclusions, hypoactivity, and severe rotarod deficits. We also compared the YAC72, HD46 and HD100 results with data gathered in 12-week-old R6/2 transgenic mice that carry a small N-terminal fragment of htt (amino acids 1–90) containing a poly(Q) tract of ~150 residues (19,44,49). The R6/2 htt fragment is coded by exon-1 of the *IT15* gene, which is expressed under the control of the *IT15* promoter.

A		R6/2 Q150 vs WT	N171 82Q vs WT	HD46 Q46 vs WT Mild	HD46 Q46 vs WT Severe	YAC72 Q72 vs WT
GenBank ID	Description					
M19436	atrial/fetal myosin alkali light chain (Myla)	-1.5	2.1	0.82	0.5	-4.3
X59520	CCK gene for cholecystokinin, exon 1	0.0	5.3	3.07	0.7	-16.2
X59520	CCK gene for cholecystokinin, exon 1	2.4	4.3	9.48	0.8	-19.9
M10114	kappa-casein mRNA	-1.2	0.2	-0.02	-1.6	-2.8
U62021	neuronal pentraxin 1 (NPTX1)	1.6	1.8	0.02	0	-4.3
U49251	putative cerebral cortex transcriptional regulator T-Brain-1	0.2	2.9	1.75	0.6	-4.2
ET61809	anti-DNA immunoglobulin heavy chain IgM antibody 373s.83	-2.4	-1.7	2.58	1.2	3.1
L01062	ATP synthase alpha subunit	1.2	-1.1	-0.07	0	23.8
X57497	glutamate receptor 1	1.2	1.0	0.02	-0.9	1.6
X06746	Krox-20 protein containing zinc fingers	-2.3	-1.7	1.33	0	4.5
X16995	N10 gene for a nuclear hormonal binding receptor	-2.1	-1.5	0.93	0.1	2.1
AA172909	similar to gb:M10062 Mouse IgE-binding factor	0.6	1.3	-0.08	-0.5	3.1
AF017630	vascular actin single-stranded DNA-binding factor 2 p44	-1.0	-1.4	0.32	-0.8	1.9
M62867	Y box transcription factor (MSY-1) mRNA	1.1	0.4	-0.12	-1.4	1.0

Figure 2. Summary of mRNA changes observed in microarray analysis of striatum and cerebellum from 12-month-old YAC72 mice. (A) Named genes that meet the $P < 0.001$ threshold upon microarray analysis of mRNA levels in 12-month-old YAC72 striatum as compared with wild-type (WT). Genes were grouped according to their general trend of altered expression in YAC72 and sorted by name. For comparison, expression of these select mRNAs in striatum of 12-week-old R6/2, 4-month-old HD N171, and 10- to 12-month-old HD46 mice (with mild or severe phenotype) is shown. The number of microarray replicates analyzed for each mouse model varied (R6/2, $N = 2$; N171, $N = 2$; HD46, $N = 6$; YAC72, $N = 2$). Within each replicate, the relative expression level of each gene in the transgenic compared to control is depicted as a colored tile (green, decreased levels; red, increased levels). The average fold change observed in transgenic compared with control is indicated to the right of the tiles. Novel mRNAs [represented only by expressed sequence tags (ESTs)] identified with altered levels at the $P < 0.001$ threshold in YAC72 striatum are not shown [AA711193 (increased in YAC72) and AA409826 (decreased in YAC72)]. (B) Named genes that meet the $P < 0.001$ threshold upon analysis of microarray mRNA levels in 12-month-old YAC72 cerebellum as compared with wild-type. Genes are depicted as in (A). For comparison, expression of these select mRNAs in cerebellum of 12-week-old R6/2, 12-month-old DRPLA At-65 and 4-month-old HD 82Q N171 mice are shown (data from 44,49). The number of microarray replicates analyzed for each mouse model varied (YAC72, $N = 5$; R6/2, $N = 2$; DRPLA, $N = 4$; N171, $N = 4$). Novel mRNAs (ESTs) increased in YAC72 cerebellum: W71831, Z31137, AA174489, AA408789, AA266033, C77300, AA671586, C76104, C76314, AA408030, AA387967, C75983, AA690583, AA542309, C76985, C76314, W65221, AA684436 and AA407085. Novel mRNA (EST) decreased in YAC72 cerebellum: W54630.

B	GenBank ID	Description	R6/2		DRPLA		N171		YAC72	
			Q150 vs WT		Q65 vs WT		Q82 vs WT		Q72 vs WT	
Y10386	C1 inhibitor.		1.2		0.7		1.1		-1.0	
AA116604	cathepsin*		1.6		-1.7		-0.2		-1.7	
X06368	c-fms proto-oncogene.		1.0		0.1		-0.8		-1.7	
X66405	collagen alpha1(VI)-collagen.		-0.3		-0.1		0.2		-0.5	
ET63118	cytochrome P450 2B10/NADPH cytochrome P450 oxidoreductase		0.1		0.2		1.1		-2.0	
AA031158	extensin precursor*		7.7		11.0		6.8		-1.5	
J04953	gelsolin gene		-1.2		-1.6		-0.7		-2.8	
V00714	gene for alpha-globin.		-1.2		-0.1		-0.5		-0.6	
M73483	glutathione S-transferase (GST Yc)		-1.1		0.3		0.0		-1.1	
U36788	holocytochrome c-type synthetase (putative)*		-1.2		-1.8		1.0		-5.0	
X00496	Ia-associated invariant chain (Ii)		3.0		0.5		0.3		-2.9	
D00613	matrix Gla protein (MGP)		-1.3		-1.1		-1.1		-1.6	
AA059700	MHC class I B(2)-microglobulin gene (W4 allele)		1.6		-0.1		-1.3		-1.6	
L00606	MHC class I Qa-1a antigen mRNA		-1.6		-0.5		0.0		-1.7	
L20315	MPS1		2.7		-1.0		-0.1		-1.2	
AA049662	plasma retinol-binding protein precursor*		0.1		-0.2		-0.5		-2.9	
X99807	selenoprotein P.		-0.2		-0.8		-0.8		-1.8	
AA124405	synaptopodin*		-1.3		-6.4		-1.4		-1.9	
W30651	translational initiation factor 2 beta*		1.2		-0.9		0.6		-1.4	
M69200	tyrosine hydroxylase		-1.2		0.7		-0.6		-0.7	
X67783	VCAM-1		-0.2		1.2		-0.1		-1.3	
AA086684	glucose regulated protein precursor (78kD)*		-1.2		-5.7		-1.0		1.7	
U73478	acidic nuclear phosphoprotein pp32		0.0		-1.1		-0.2		1.3	
AA114623	ankyrin, brain variant 2*		0.0		-0.1		-0.1		1.8	
AA108330	astrocytic phosphoprotein, PEA-15		1.5		-1.5		-0.7		2.1	
U03184	cortactin		1.6		-1.1		1.2		1.5	
U03279	phosphatidylinositol 3-kinase 110 kDa subunit		1.2		-0.8		0.0		1.5	
D37791	beta-1,4-galactosyltransferase		-0.1		1.3		0.6		1.7	
U04827	brain fatty acid-binding protein		1.7		0.7		0.6		1.1	
X55573	brain-derived neurotrophic factor		-3.2		-3.3		-4.3		1.9	
X71788	Burkitt lymphoma receptor 1 homologue.		-2.4		-0.3		0.0		2.4	
AA153484	calcium-transporting ATPase sarcoplasmic reticulum type (SERCA2)*		-1.8		-3.5		-1.2		2.0	
U39904	citron, putative rho/rac effector		0.0		1.7		1.8		2.0	
AF000998	Clock		1.6		-1.7		0.1		0.9	
W54784	creatine kinase, B chain*		-1.3		-1.5		-1.2		1.6	
W10047	DNA topoisomerase I*		1.2		0.8		1.1		1.0	
U32329	endothelin-B receptor (EDNRB)		-2.0		-1.5		-0.7		1.9	
C80644	eukaryotic initiation factor 4 gamma (eIF-4)*		-0.3		-1.3		0.0		1.6	
AA038437	eukaryotic initiation factor 4 gamma (EIF-4-GAMMA)*		1.3		0.1		-0.6		1.6	
W61845	gamma enolase (neural)*		-1.3		-2.1		-1.7		1.2	
D78645	glucose regulated protein precursor (78kD)		-0.1		-1.4		-0.5		1.5	
U20344	gut-enriched Kruppel-like factor GKL		-1.4		0.6		-1.3		2.0	
AA050397	heat shock cognate (71kD)*		0.0		-0.9		-0.5		1.1	
M12572	heat shock protein (hsp68)		-2.2		1.8		-0.6		3.4	
D12907	heat shock protein (HSP47)		-1.3		0.6		-1.3		1.4	
AB005141	klotho		1.9		4.7		2.7		4.3	
D84391	L1 repetitive element		-1.2		-1.5		-0.6		1.7	
X80417	MB-IRK2		1.3		-1.2		-0.8		0.7	
U54984	membrane-type matrix metalloproteinase 1		-1.3		0.8		-0.7		1.5	
AA028730	myosin 10 chain alkali, non-muscle isoform*		0.0		0.1		-1.3		1.6	
D17571	NADPH-cytochrome P450 oxidoreductase		-1.1		0.9		0.6		1.1	
U83148	NFIL3/E4BP4 transcription factor		0.2		0.7		0.7		1.0	
ET63083	PR264		0.3		1.9		-2.4		1.9	
U28423	protein kinase inhibitor p58		0.2		0.3		0.6		1.5	
AF022992	Rigui		-2.1		0.2		-1.7		1.1	
D67076	secretory protein containing thrombospondin motifs		-1.1		-2.0		-0.1		1.6	
AA037987	serine/threonine protein phosphatase PP1*		-1.2		-0.4		-0.8		1.2	
U86783	Nurr1, steroid/thyroid hormone orphan nuclear receptor		-11.4		-2.5		-2.2		4.5	
X66402	stromelysin 1		-0.1		-0.8		0.3		2.9	
W75918	transcriptional regulatory protein RPD3*		1.1		-0.8		-1.3		1.6	
M25149	Tum-P91A antigen		1.7		-0.1		1.3		1.3	
AF027963	X box binding protein-1 (XBP-1)		-1.1		0.6		-1.2		1.1	
W62091	Xeroderma pigmentosum group E protein*		1.2		-0.1		1.2		1.4	
W42234	Xeroderma pigmentosum group E protein*		2.2		-0.5		0.7		1.8	

* sequence similar to named gene

Figure 2. continued

changes in cell culture systems (40–42) and yeast (43). Since these alterations in mRNA levels can be detected on an mRNA per cell basis, they appear to arise from cellular changes in gene expression rather than from gross neuronal loss.

Recently, we identified a set of gene expression changes common to five mouse models of poly(Q) disease (44). These shared mRNA changes suggested to us that some poly(Q)-related changes in gene expression could occur independently of protein context. Surprisingly, these changes were not observed in corresponding brain samples from transgenic mice expressing full-length mutant htt. This finding suggested that length of the htt protein could modulate the ability of its expanded poly(Q) domain to alter gene expression. Here, we investigated whether htt protein context can reduce the effects of expanded poly(Q) on gene expression by assessing mRNA levels in transgenic mice that express the N-terminal one-third or full-length version of mutant htt.

The lines of mice employed in the current study have been described previously. HD46 mice (lines 14 and 17) and HD100 mice (line 49) express the N-terminal one-third (964 amino acids) of htt with either 46 or 100 glutamine residues (45). HD46 and HD100 mice display htt accumulation and aggregates in the striatum and cerebral cortex. Striatal neurons in HD100 mice demonstrate impaired responsiveness to cortical stimulation. Behaviorally, these animals have impaired rotarod performance, exhibit clasping and demonstrate gait abnormalities. We also analyzed mice YAC72 transgenic mouse (line 2511) that expresses full-length htt with a 72 residue poly(Q) tract (22). By 6–7 months of age, YAC72 mice display behavioral hyperactivity and enhanced long-term potentiation in the hippocampus. By 9 months of age, decreased levels of brain-derived neurotrophic factor (BDNF) are observed in the striatum, cortex and hippocampus of YAC72 mice (46). By 12 months of age, YAC72 mice display striatal neuronal pathology, including nuclear htt accumulation, hyperchromasia, chromatin condensation, mitochondrial swelling and neurodegeneration. In addition, striatal medium spiny neurons in YAC72 mice of ages ranging from 6 months to 2 years display enhanced responses to NMDA (47,48). The relative sizes of the htt transproteins investigated in this study are shown in Figure 1.

Here, we report that brain tissues of HD46, HD100 and YAC72 mice exhibit fewer gene expression changes than corresponding tissues of mice that express shorter N-terminal mutant htt fragments. Further, mRNAs that are consistently decreased in multiple poly(Q) disease mouse models or human HD patients were generally present at normal levels in HD46, HD100 and YAC72 mice. Thus, htt protein context appears to have a dramatic influence on the poly(Q)-related disruption of

mRNA expression. Taken together with previous studies, our results suggest that the effects of mutant htt on gene expression in the brain occur *after* its proteolysis to shorter N-terminal fragments.

RESULTS

Microarray analysis of striata from HD46 and YAC72 mice

To explore altered gene expression globally, striatal mRNAs of YAC72 and HD46 transgenic mice were analyzed using oligonucleotide microarrays. These studies were performed within the Hereditary Disease Array Group (HDAG), which utilized a single core microarray facility and single microarray platform. This facilitated comparisons between different poly(Q) disease models by standardizing experimental design, quality control and data analysis (50).

RNA samples were prepared from striatal tissues of 12-month-old YAC72 and 10- to 12-month-old HD46 transgenic mice (with *Mild* or *Severe* symptoms as defined in Materials and Methods) in addition to age- and strain-matched wild-type controls. Microarray data were analyzed using custom-designed statistical algorithms that incorporate error modeling (51). For each experiment, we determined the number of differentially expressed mRNAs that passed the $P < 0.001$ threshold. Fifteen to twenty mRNAs passed this threshold in analyses of HD46 versus control and YAC72 versus control striata (Table 1). These numbers of mRNAs are only slightly higher than the predicted number of false-positive determinations (i.e. 1:1000, as defined by the P -value criterion). With the use of the same statistical algorithm, 147 mRNAs were differentially detected in 12-week-old R6/2 striatum versus control. These data clearly demonstrate that striatal gene expression changes are significantly more subtle in YAC72 and HD46 mice than in R6/2 mice—at least in mice of these particular ages.

Differentially detected mRNAs meeting the $P < 0.001$ threshold in 12-month-old YAC72 striatum are listed in Figure 2A. There was no overlap between the mRNAs that were differentially detected in YAC72 striatum by microarray ($P < 0.001$) and those differentially detected in 12-week-old R6/2 mice or 4-month-old N171-82Q HD mice, which express amino acid residues 1–171 of mutant htt with an 82-residue poly(Q) tract (23). Microarray analyses of striata from symptomatic R6/2 and N171-82Q mice were performed within the HDAG and are reported in full elsewhere (39,44,49).

Table 1. Numbers of genes meeting the $P < 0.001$ threshold in microarray analyses of striata from HD46 mild, HD46 severe, YAC72 and R6/2 mice

	HD46 mild versus WT	HD46 severe versus WT	YAC72 versus WT	R6/2 versus WT
Age	10–12 months	10–12 months	12 months	12 weeks
Replicates (WT/TG)	2/2	2/2	2/2	2/2
mRNAs at $P < 0.001$	15	20	16	147

Each microarray data analysis was performed with $N = 2$ transgenic replicates and $N = 2$ age- and strain-matched wild-type replicates. HD46 and YAC72 animals were analyzed at ~1 year of age. R6/2 mice were analyzed at 12 weeks of age as described in (49). $P < 0.001$ criteria are described in the text. WT, wild-type; TG, transgenic.

To increase the statistical power of our microarray analysis, we increased the number of replicate HD46 samples to six per group. Lists of mRNAs with altered levels ($P < 0.001$) in HD46 *Mild* and *Severe* mice are provided in supplemental data (www.neumetrix.info). HD46 microarray data for mRNAs corresponding to those identified in analyses of YAC72 striata are also shown in Figure 2A. The only mRNAs that meet the $P < 0.001$ threshold in analyses of striatum from YAC72 and either *Mild* or *Severe* HD46 mice are N10 (increased in YAC72 and HD46 *Mild*, decreased in R6/2 and N171-82Q) and cholecystokinin (decreased in YAC72, trend toward decrease in R6/2, increased in HD46 *Mild* and N171-82Q). As described below, the confirmation rate of the $N = 6$ microarray analysis was low, suggesting that the inability to detect mRNA changes was a true reflection of the HD46 molecular phenotype and not due to limited statistical power.

Cerebellar gene expression changes in YAC72 mice

The results above indicated that mRNA changes were subtle in striata of mice expressing a large N-terminal portion or full-length form of mutant htt. To determine whether this finding was unique to the striatum, we performed microarray analyses of cerebella from 12-month-old YAC72 and control mice. For reference, we drew comparisons with cerebellar data gathered from N171-82Q HD mice. The cerebellar N171-82Q microarray data set was gathered with similar power ($N = 4-5$ per group) (44). The YAC72 cerebellum displayed fewer mRNA alterations at any statistical threshold than the N171-82Q cerebellum (e.g. at $P < 0.001$, YAC72 = 84 genes; N171 = 165 genes, predicted false-positives = 13 for each). Furthermore, the magnitudes of mRNA change (average fold change) were much smaller in YAC72 than in N171-82Q or R6/2 mice. Named mRNAs that showed altered levels in YAC72 cerebellum compared with control are summarized in Figure 2B. Comparison of mRNA alterations in YAC72 cerebellum with other poly(Q) disease models revealed that most of the transcripts that were differentially detected in YAC72 mice did not show similarly altered levels in cerebella of R6/2, N171-82Q and 12-month-old At-65Q (atrophin-1 transgenic) (52) mice (data from ref. 44). Conversely, the

expanded poly(Q)-mediated cerebellar mRNA alterations observed in the R6/2 and N171-82Q mice (44) were not observed in the cerebellum of YAC72 mice. Thus, the mRNA alterations present in YAC72 cerebellum appear to be both more restricted and distinct from those caused by expanded poly(Q) within the short htt transproteins of R6/2 and N171-82Q mice.

Confirmation of microarray data in YAC72 and HD46 mice

Selected mRNAs that were differentially detected in microarray analyses were evaluated by northern analysis or quantitative RT-PCR using the original RNA samples assayed by microarray. All confirmation data are summarized in Table 2. In YAC72 striatal samples, RT-PCR confirmed increased levels of N10 and Krox 20 mRNAs ($P < 0.02$; Fig. 3A). A putative decrease in pentraxin-1 mRNA in striatum could not be confirmed. In YAC72 cerebellar samples, RT-PCR confirmed a statistically significant decrease in cytochrome *c* synthase mRNA levels ($P < 0.0001$), while levels of brain-derived neurotrophic factor (BDNF) and cathepsin mRNAs were not significantly different between YAC72 and control mice (Fig. 3B).

In striatal samples from HD46 mice, candidate mRNA changes could not be confirmed for creatine kinase, dopamine D2 receptor or neuronal protein NP25 (Fig. 3C). Overall, the low confirmation rate observed for the HD46 and YAC72 microarray data is consistent with the high predicted false-discovery rate.

Anatomic analyses of candidate mRNAs in HD46, HD100 and YAC72 mice

As stated above, gene expression changes that are observed in the HD R6/2 and N171-82Q mouse models were not detected in HD46, HD100 or YAC72 mice. Because this finding was unexpected, we wished to rule out possible causes of false-negative results (e.g. regional heterogeneity within striatum). Therefore, we extended our studies to include radioligand-binding assays and *in situ* hybridization histochemistry, both of which retain anatomic integrity. We focused on neurotransmitter receptors, adenylyl cyclase, DARPP-32, the 11S proteasome

Table 2. Summary from confirmation studies in HD46 striatum, YAC72 striatum and YAC72 cerebellum

mRNA	HD46 mild striatum	Assay	N (WT/TG)	P	HD46 severe striatum	Assay	N (WT/TG)	P
NP25	85%	Northern	6/6	0.161	78%	Northern	6/6	0.045
Creatine kinase B	130%	Northern	4/7	0.251	128%	Northern	4/6	0.272
Dopamine D2 receptor	145%	Northern	4/7	0.108	125%	Northern	4/6	0.700
	YAC72 striatum							
N10	192%	RT-PCR	3/3	<0.02				
Krox20	216%	RT-PCR	3/3	<0.01				
Pentraxin-1	53%	RT-PCR	3/3	0.234				
	YAC72 cerebellum							
BDNF	137%	Northern	6/6	0.407				
Cathepsin	127%	Northern	6/6	0.107				
Cytochrome <i>c</i> synthase	156%	RT-PCR	4/4	<0.0001				

RNA samples originally analyzed by microarray were used in northern or quantitative RT-PCR confirmation studies. mRNA levels are expressed as percentage of age- and strain-matched wild-type controls. The number of wild-type (WT) and transgenic (TG) replicates and the calculated P -value are indicated for each experiment.

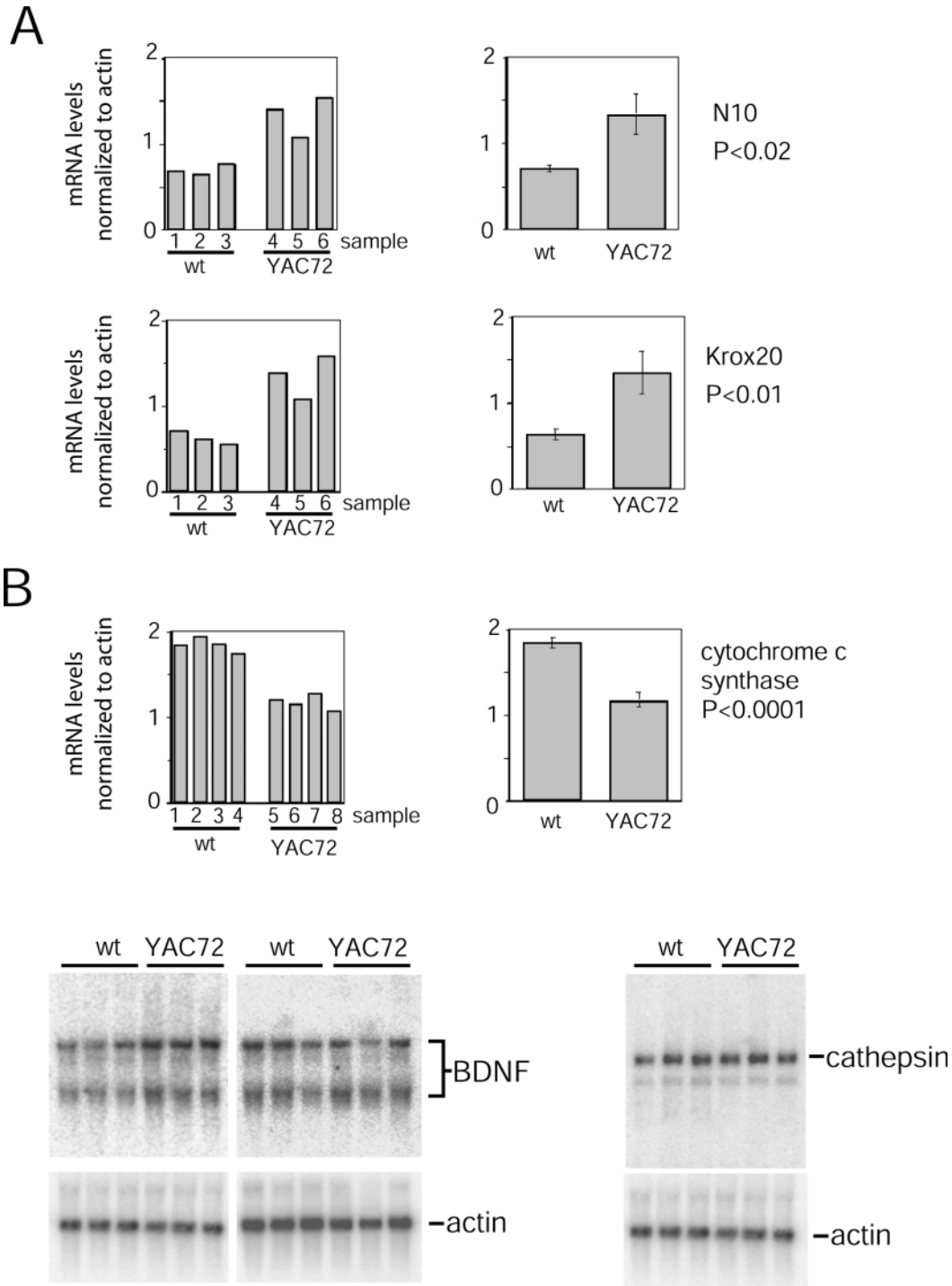


Figure 3. Confirmation of candidate genes identified by microarrays. All confirmatory experiments were performed on RNA samples originally analyzed by microarray. **(A)** Representative confirmatory studies on YAC72 striatal samples. Real-time quantitative PCR was performed using $N = 3$ wild-type (wt) and $N = 3$ YAC72 samples derived from mice at 12 months of age. All PCR values are expressed as relative mRNA levels normalized to β -actin mRNA levels measured in the same sample. The left panels show normalized mRNA levels in individual wild-type and transgenic samples. The right panels show average of each genotype group \pm SD. For candidate mRNAs N10 and Krox20, significantly altered expression was demonstrated (at least $P < 0.02$). **(B)** Representative confirmatory studies on YAC72 cerebellar RNA samples derived from mice at 12 months of age. Quantitative RT-PCR confirmed at $P < 0.0001$ decreased levels of cytochrome *c* synthase mRNA using $N = 4$ wild-type and $N = 4$ YAC72 cerebellar RNA samples derived from mice at 12 months of age. Brain-derived neurotrophic factor (BDNF) and cathepsin mRNAs were not significantly different between YAC72 and control (see also Table 2). **(C)** Representative confirmatory studies on HD46 striatal samples. Northern analyses were performed on RNA samples gathered from individual HD46 mice at 10–13 months of age. HD46 mice were from either line 14 or line 17 and were categorized with either mild or severe (sev) phenotypes. Levels of neuronal protein NP25, creatine kinase (CK) and dopamine D2 receptor (D2r) mRNAs measured by northern analysis were not consistent with the array results. Membranes were reprobbed to document β -actin mRNA levels. The band below β -actin in the creatine kinase control blot is residual signal from a preproenkephalin radioprobe hybridized to the membrane. See also Table 2.

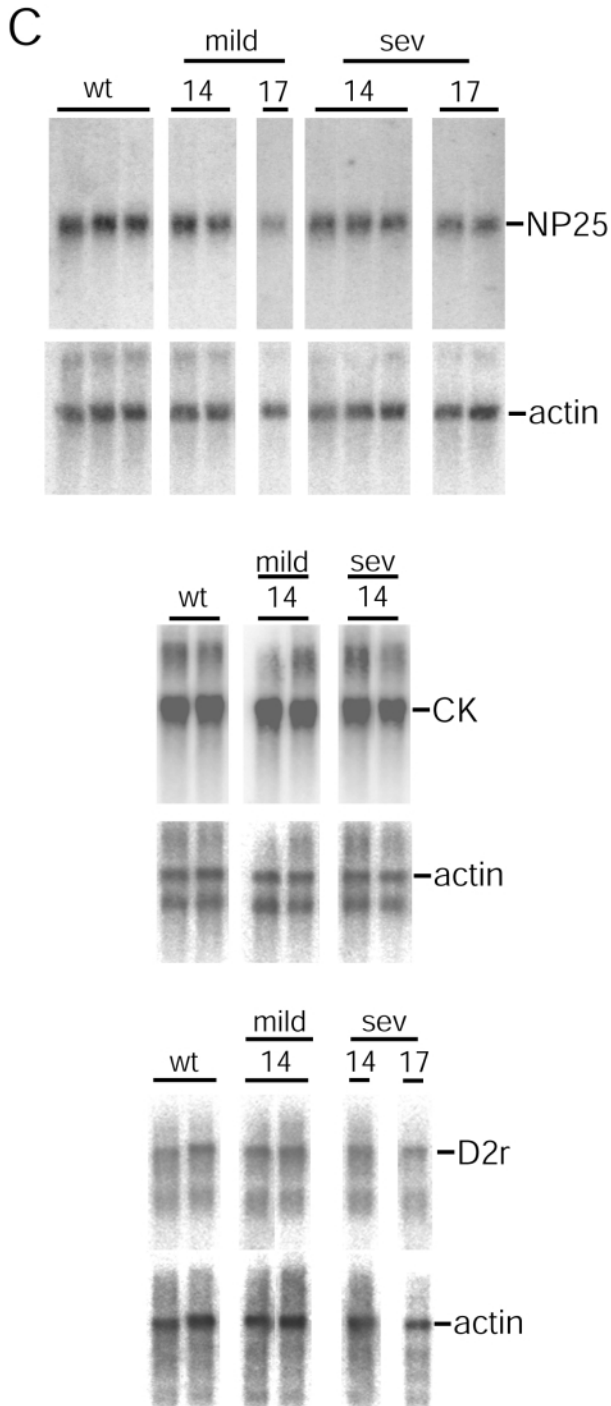


Figure 3. continued

activator α subunit (PA28 α) and preproenkephalin because these were shown previously to be decreased in multiple mouse and/or human HD tissues (34–39). HD46, HD100 and YAC72 mice were studied at ages when neurologic phenotypes were detectable. No significant changes in the levels of DARPP-32, PA28 α , preproenkephalin, NMDA receptor or adenosine A2a receptor mRNAs could be detected in the striatum of 12-month-old YAC72 mice as compared with age-matched

wild-type controls (Fig. 4A and Table 3). Likewise, no significant changes in binding to adenylyl cyclase, group I or group II metabotropic glutamate receptors or muscarinic acetylcholine receptors were detected in the striatum of YAC72 mice (Fig. 4B and Table 3).

We similarly analyzed brain sections of HD46 and HD100 mice at 10–13 months of age. We observed no significant differences in preproenkephalin mRNA levels within the striatum of HD46 or HD100 mice as compared with wild-type controls (Fig. 4C and Table 3). The only abnormalities observed in these animals that recapitulated findings in other HD mice and HD patients were decreased levels of adenosine A2a receptor mRNA and decreased dopamine D2 receptor binding, which were selectively observed in the HD100 but not the HD46 mice. Unexpectedly, we detected increased mRNA levels for dopamine D1 receptor in the striatum of HD46 and HD100 mice—a finding *opposite* to that observed in HD patients and mice expressing shorter N-terminal fragments of mutant htt. These observations demonstrate that the gene expression changes in HD46 and HD100 mice are lower in magnitude and scope as compared with the R6/2 N-terminal htt transgenic mice. Importantly, however, the observed decreases in adenosine and dopamine receptors indicate that 10- to 13-month-old HD100 mice may be starting to manifest the transcriptional dysregulation evidenced in HD brain. Overall, the absence of mRNA or neurotransmitter receptor binding changes in YAC72 brain is highly consistent with microarray findings, supporting the hypothesis that htt protein length in excess of 171 N-terminal residues limits the ability of expanded poly(Q) to alter gene expression.

DISCUSSION

Overall, HD46, HD100 and YAC72 mice expressing extended N-terminal or full-length forms of mutant htt display subtler and qualitatively different gene expression changes than mouse models that express shorter N-terminal fragments of mutant htt. Messenger RNA (or corresponding protein) levels for specific molecular markers such as neurotransmitter receptors were analyzed in HD46, HD100 and YAC72 mice using standard assays established previously in our laboratories (37–39). Except for modest decreases in dopamine D2 receptor binding and A2a receptor mRNA in HD100 mice, even the most dramatic gene expression changes observed in other HD transgenic mice were absent in mice expressing the relatively longer and full-length mutant htt transproteins. Lower levels of transcriptional dysregulation in HD46 and YAC72 mice were also detected by microarray profiling. Although it is possible that gene expression changes may be present in a small subset of cells within HD46 and YAC72 brain tissues that eluded detection by the methods employed, it is clear that the majority of cells do not show large shifts in mRNA levels.

We examined HD46, HD100 and YAC72 mice at ages when poly(Q) disease signs were already present (22,45,46,48). Thus, our results show that large-scale perturbations in mRNA levels are not required for the development of the neurologic phenotypes observed in these HD animal models. A reasonable interpretation of this finding is that large-scale gene expression

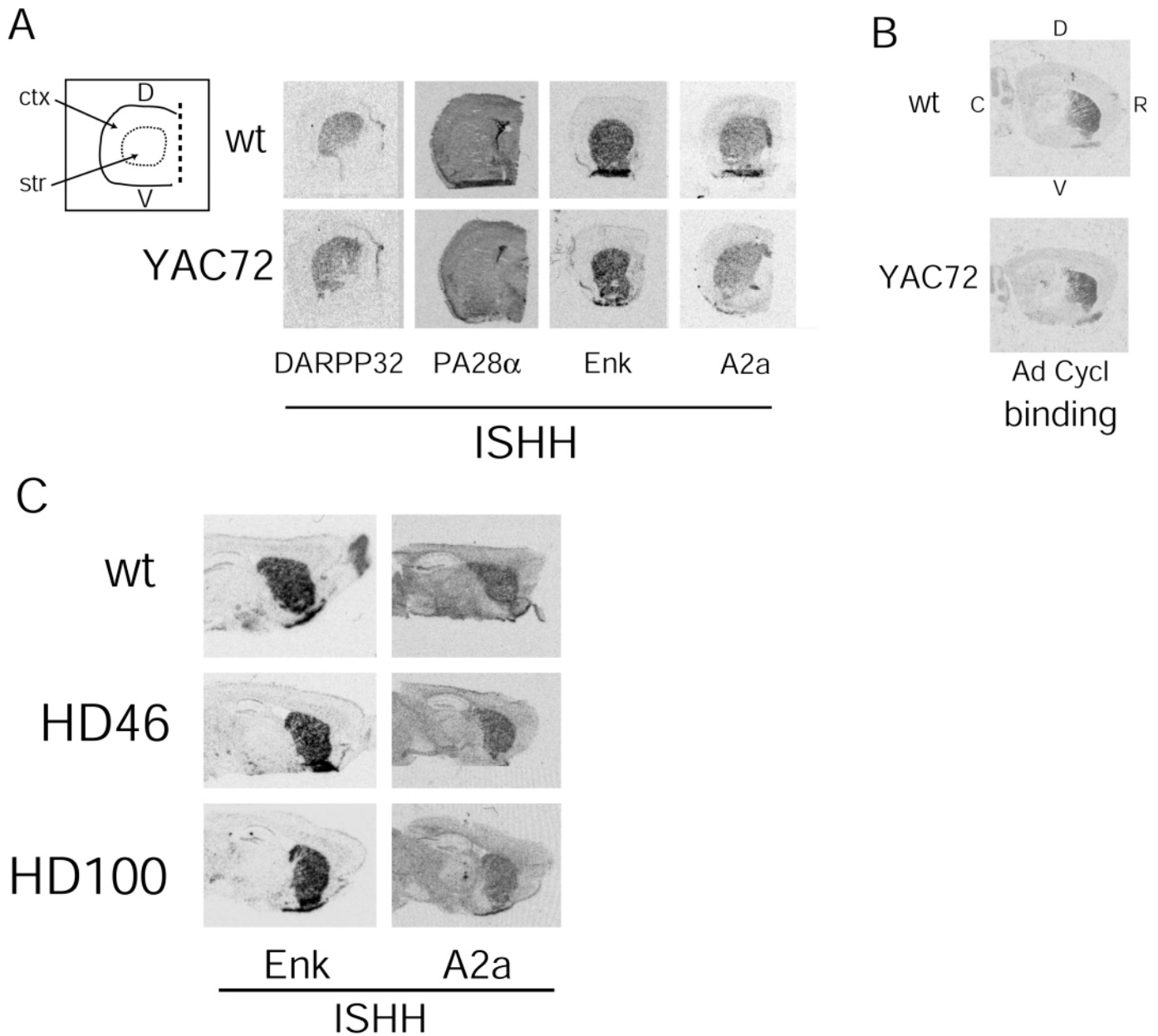


Figure 4. *In situ* hybridization and ligand binding analyses for marker genes in HD46, HD100 and YAC72 brain. **(A)** and **(B)** show representative data gathered using brain coronal (A) or sagittal (B) sections of 12-month-old YAC72 and wild-type (wt) control mice. **(A)** Left: the orientation of the coronal section is depicted in a line diagram showing the bisecting plane, dorsal (D) and ventral (V) surfaces, and the relative locations of the cortex (ctx) and striatum (str). Right: as detected by *in situ* hybridization histochemistry (ISHH), no differences in DARPP32, 11S proteasome activator α subunit (PA28 α), preproenkephalin (Enk) or adenosine A2a receptor (A2a) mRNAs were observed in YAC72 striatum (see also Table 3). **(B)** No changes in the binding of radiolabeled forskolin to adenylyl cyclase (Ad Cycl) could be detected in striatum of YAC72 mice. Orientation of sagittal section is indicated in the wild-type (wt) panel: C, caudal; R, rostral; D, dorsal; V, ventral. (See also Table 3.) **(C)** Representative autoradiograms of sagittal brain sections of 10- to 13-month-old HD46, HD100 and wild-type (wt) control mice. The orientation of sagittal sections is as in (B). Preproenkephalin (Enk) mRNA was not significantly different between HD46 or HD100 mice and controls by ISHH. Adenosine A2a receptor (A2a) mRNA was slightly decreased in striatum of HD100 mice compared to controls. (See also Table 3.)

changes in the striatum are not an integral component of the early stages in HD pathogenesis. Data from young R6/2 mice (<6 weeks of age) also support this conclusion (44). In addition, our data suggest that the behavioral, electrophysiologic and neuropathologic abnormalities identified in YAC72, HD46 and HD100 mice represent earlier disease stages which precede overt transcriptional dysregulation. Since most neurotransmitter

receptor decreases identified in grade 0 HD postmortem brain were not present in HD46, HD100 and YAC72 mice, the stages of disease progression in these animals (up to ~12 months of age) may best model HD brain with neuropathology less severe than grade 0.

Based on this projected timeline, we predict that more pronounced gene expression changes will take place in the

Table 3. Summary from analyses of marker gene expression in striatum of YAC72, HD46 and HD100 mice

mRNA or protein	YAC72	Assay	N (WT/TG)	P	HD46 mild	Assay	N (WT/TG)	P	HD46 severe	Assay	N (WT/TG)	P	HD100	Assay	N (WT/TG)	P	R6/2	Assay	Ref.
Preproenkephalin	111.0%	ISHH	3/3	0.239	98.5% ^a	ISHH	4/6	0.876 ^a					95.0%	ISHH	4/5	0.658	21.0%	ISHH	39
	93.9%	RT-PCR	4/4	>0.05	103.0%	Northern	4/7	0.750	131%	Northern	4/7	0.400	ND				31.0%	Northern	<i>P</i> = 0.0242
DARPP32	86.0%	ISHH	3/3	>0.05	ND				ND				ND				33.0%	ISHH	39
PA28 α	107.0%	ISHH	3/3	>0.05	ND				ND				ND				269.0%	Northern	39
zif268	121.4%	RT-PCR	4/4	>0.05	ND				ND				ND				21.0%	Northern	39
Dopamine D1 receptor	ND				136.0% ^a	Binding	4/6	0.017 ^a					133.0%	Binding	4/6	0.028	37.7%	ISHH	37
Dopamine D2 receptor	ND				92.0% ^a	Binding	4/6	0.230 ^a					72.0%	Binding	4/6	0.001	39.0%	ISHH	37
Adenosine A2a receptor	ND				145.0%	Northern	4/7	0.108	125%	Northern	4/6	0.700	ND				48.7%	Northern	<i>P</i> = 0.0086
NMDA receptor1	100.0%	ISHH	3/3	0.948	107.0% ^a	ISHH	4/6	0.170 ^a					84.8%	ISHH	4/5	0.010	31.8% ^b	ISHH	38
NMDA receptor2a	113.0%	ISHH	5/8	0.290	ND				ND				ND				105.0%	ISHH	37
NMDA receptor2b	102.0%	ISHH	5/8	0.890	ND				ND				ND				ND		
Adenylyl cyclase	119.0%	ISHH	5/8	0.160	ND				ND				ND				ND		
Group I mGlutamate receptor	103.0%	Binding	5/8	0.830	ND				ND				ND				24.0%	Binding	39
Group II mGlutamate receptor	117.0%	Binding	4/4	0.600	ND				ND				ND				61.1%	Binding	37
mAcetylcholine receptor	104.0%	Binding	4/4	0.710	ND				ND				ND				72.6%	Binding	37
	101.0%	Binding	4/4	0.750	ND				ND				ND				64.7%	Binding	37

Brain sections or RNA samples from 12 month-old YAC72 and 10-13 month-old HD46 and HD100 mice were analyzed by either *in situ* hybridization histochemistry (ISHH), radiolabeled ligand binding, Northern blot, or quantitative RT-PCR. Expression levels are presented as percentage of age- and strain- matched wild-type controls. The number of wild-type (WT) and transgenic (TG) samples and the calculated *P*-value are indicated for each experiment. For reference, previous observations using the same assays on samples from 12 week-old R6/2 mice are included. Data presented with *P*-values were collected in the present study. ND, not determined.

^aData from HD46 mild and severe are combined.

^bAnalysis of 8-week-old R6/2 and control mice.

striatum of HD46, HD100 and YAC72 mice at ages older than those studied here (limitations of a mouse's lifespan notwithstanding). The mild decreases in dopamine D2 and adenosine A2a receptors that already present in 10- to 13-month-old HD100 mice are consistent with a possible time and poly(Q) length-dependent pathogenic progression, since these receptor subclasses were described to comprise some of the earliest receptor decreases in grade 0 postmortem HD brain (53).

Multiple reports have demonstrated that R6/2 mice recapitulate many mRNA changes seen in HD patients (37–39). Here, we conclude that increased length of the htt transproteins leads to decreased transcriptional dysregulation in HD46, HD100 and YAC72 mice as compared with R6/2 and N171 mice. Taken together, the results suggest that short N-terminal fragments of mutant htt may be the true culprit underlying the abnormal gene expression observed in HD patient brain. Given the limited huntingtin context sequences in the N-terminal htt fragments of the R6/2 and N171 transproteins, it is plausible that some of these gene expression changes result from generalized poly(Q) effects (44,49).

There are several possible explanations for the apparent inverse relationship between htt protein length and transcriptional dysregulation. Mutant htt is believed to cause gene expression changes through direct interactions with transcriptional regulators, and most of the transcription factors known to associate with htt involve domains present in the exon 1-encoded N-terminal htt fragment (26–29,33). While both full-length and truncated huntingtin proteins can bind to these interacting proteins, other unique properties of the N-terminal fragment may explain its potency in dysregulating gene expression. First, short N-terminal htt fragments have an enhanced nuclear distribution (6). Although, nuclear htt immunoreactivity has been documented in HD46, HD100 (45) and YAC72 mice (22), the nuclear concentrations reached in these cases are likely to be lower than those found in R6/2 mice that express solely the short N-terminal fragment. Enhanced nuclear concentration of htt would increase its access to transcription factors at or near their site of action, possibly even while bound to DNA. Second, shorter fragments of mutant htt have a higher rate of aggregation *in vitro* (54) and *in vivo* (21). Thus, short N-terminal htt fragments may also have an enhanced capacity to entrap transcriptional regulators into aggregates.

Conversely, one may consider protective effects afforded by htt protein context. The simplest would invoke steric hindrance; C-terminal regions of htt could 'hide' the toxic poly(Q) stretch. Alternatively, a protective function or interaction requiring the unique C-terminal sequences of htt could be lost after the protein is cleaved. Full-length wild-type htt has been shown to protect against poly(Q)-mediated toxicity in mice (55), and cell culture data have indicated that domains with some protective function reside even within the N-terminal 548 amino acid residues of htt (56). Possibly, loss of a protective effect provided by htt sequences C-terminal to amino acid 171 could, thus, result in secondary changes that lead to altered gene expression.

Transcription-related abnormalities may be one of several parallel pathways involved in htt-mediated cellular dysfunction. The results of the present study suggest that short N-terminal fragments of mutant htt are important molecular intermediates

for HD-related disruptions in gene expression. Further, our results suggest that large-scale alterations in gene expression occur later in disease progression than other abnormalities that have already been identified in mouse models expressing 'large' or full-length versions of mutant htt. Based on our conclusions, we predict that inhibition of htt proteolysis into shorter more toxic fragments might slow the later stages of progression and represent a potential HD therapeutic strategy. This approach would only be viable, however, if proteolytic processing of htt could be inhibited in a way that did not interfere with its normal function in the cell.

MATERIALS AND METHODS

Mice

HD46 and HD100 animals, which express amino acid residues 1–964 of htt under control of the *neuron-specific enolase* (NSE) promoter, were assessed for severity of disease phenotype and assigned a hazard score as described previously (45). Animals defined as showing a 'severe' phenotype exhibited clasping and rotorod impairment, whereas these deficits were absent in mice defined as having a 'mild' phenotype.

YAC72 mice and sex-matched wild-type FVB/N mice were analyzed at 12 months of age. For each YAC72 mouse, genotypes and equivalent expression of mutant htt transprotein were confirmed using cortical tissue (see supplemental data at www.neumetrix.info).

Mice were sacrificed by cervical dislocation and brains were removed immediately. Whole brains for histologic studies were frozen in an isopentane bath on dry ice. For RNA extractions, striatal and/or cerebellar tissues were dissected and snap-frozen on dry ice. Within each experiment (YAC72 or HD46), all dissections were performed by the same investigator. Tissues were stored at -80°C until processed.

RNA isolation and preparation of microarray samples

Total RNA was isolated from striata and cerebella by extraction with TRI-Reagent (Sigma-Aldrich; HD46 samples) or Trizol (Invitrogen; YAC samples). For striatal samples, total RNA was purified further over RNeasy columns (Qiagen). For the striatal microarray analyses, 15 μg of total RNA was pooled for each sample. For YAC striatal samples ($N=2$ transgenic, $N=2$ wild-type), 7.5 μg of total RNA from each of two mice was pooled; for HD46 samples [$N=6$ wild-type, $N=6$ mild (4 from line 17, 2 from line 14), and $N=6$ severe (4 from line 17, 2 from line 14)], RNA was taken from one or two animals. For striatal samples, labeled cRNA probes were generated from total RNA samples according to the Affymetrix GeneChip protocol.

For the YAC72 cerebellar samples, poly(A)⁺ RNA was purified from total RNA (extracted from a single YAC72 or wild-type cerebellum) using the Oligotex mRNA isolation system (Qiagen). Cerebella from $N=5$ YAC72 and $N=5$ wild-type mice were analyzed. Labeled cRNA probes were

generated from half of each poly(A)⁺ RNA sample according to the manufacturer's protocol (Affymetrix).

Biotinylated cRNA probes were hybridized to Murine 11K oligonucleotide microarrays (chip B first and then chip A) using the Affymetrix Fluidics Station 400 according to the manufacturer's standard protocol.

***In situ* hybridization and ligand-binding histochemistry**

ISHH assays were performed as described in (37,38) for the adenosine A2a receptor and NMDA receptors and in (39) for preproenkephalin, DARPP32 and PA28 α . In YAC72 studies, ISHH signals for target mRNAs were normalized to actin mRNA measured in adjacent brain sections. Ligand binding assays were carried out as described in (39) for adenylyl cyclase and in (37,38) for neurotransmitter receptors.

Northern blotting

Northern analyses were used to quantitate mRNA levels in HD46 samples as described previously (39). To control for variations in sample loading, target mRNA intensities were normalized to β -actin mRNA (the sequence and use of the actin probe are described in 49).

Real-time quantitative RT-PCR

First-strand cDNA was prepared from 2 μ g of total RNA using Superscript II (Invitrogen) in a final volume of 20 μ l according to the manufacturer's protocol. After incubation of first-strand reaction at 42°C for 1 h, samples were heated at 100°C for 3 min and brought to a volume of 200 μ l total with water. These RT reactions (2 μ l) were used as template in real-time PCR reactions. Real-time PCR was performed by SYBR green two-step RT-PCR (Roche Biochemical and Applied Biosystems). Serially diluted cDNA samples were used for standard curve calibration. For all primer sets, we confirmed that less than 0.5% of the quantitative signal was detected when negative control RT reactions (without Superscript enzyme) were substituted for cDNA template. Expression changes were normalized to β -actin mRNA levels measured in parallel. Primary data analysis was performed using system software from Roche Biochemical or Applied Biosystems as recommended by the manufacturer. We confirmed in preliminary control experiments that differences in mRNA levels detected by real-time PCR were comparable to differences documented in the same samples using northern blotting (see supplemental data at www.neumetrix.info).

ACKNOWLEDGEMENTS

The authors thank R.E. Hughes, K. Kegel, G. Yohrling and E. Signer for critical reading of the manuscript. They thank Y. Kaneko, K. Blankson, L. Farrell, J. Kuster and N. Peters for excellent technical support. The authors would also like to thank the Hereditary Disease Array Group, the Microarray Facility at the Fred Hutchinson Cancer Research Center and Affymetrix for assistance and support with microarray experiments. The data repository at www.neumetrix.info was

generously developed by 3rd Millennium (Cambridge, MA). Data for N171-82Q and At-65Q mice were graciously shared with us by G. Schilling, C.A. Ross and D.R. Borchelt.

This work was supported by grants from the US National Institutes of Health to A.B.Y. (AG13617), R.L.-C. (NS10800), J.-H.J.C. (NS38106), M.D. (NS35711 and NS16367) N.A. (NS38194) and J.M.O. (NS42157). This work was also supported by grants from the US Department of Defense to N.A. (USAMRMC 98292059).

E.Y.W.C. is supported by fellowships from the Canadian Institutes of Health Research (CIHR), Huntington Society of Canada and the Michael Smith Foundation for Medical Research. B.R.L. is supported by a CIHR Clinician-Scientist award. M.R.H. is supported by the CIHR and Canadian Networks of Centers of Excellence, and is a holder of a Canada Research Chair. A.B.Y. and J.-H.J.C. are recipients of awards from the Glendorn Foundation. R.L.-C., A.B.Y., J.M.O., M.D., N.A., B.R.L. and M.R.H. are recipients of awards from the Cure HD Initiative of the Hereditary Disease Foundation. M.R.H., M.D. and J.-H.J.C. are recipients of awards from the Huntington's Disease Society of America Coalition for the Cure. N.A. is a recipient of the University of Massachusetts institutional award.

REFERENCES

- Huntington's Disease Collaborative Research Group. (1993) A novel gene containing a trinucleotide repeat that is unstable in Huntington's disease chromosomes. *Cell*, **72**, 971-983.
- Vonsattel, J.P., Myers, R.H., Stevens, T.J., Ferrante, R.J., Bird, E.D. and Richardson, E.P. (1985) Neuropathological classification of Huntington's disease. *J. Neuropathol. Exp. Neurol.*, **44**, 559-577.
- Graveland, G.A., Williams, R.S. and DiFiglia, M. (1985) Evidence for degenerative and regenerative changes in neostriatal spiny neurons in Huntington's disease. *Science*, **227**, 770-773.
- Reiner, A., Albin, R.L., Anderson, K.D., D'Amato, C.J., Penney, J.B. and Young, A.B. (1988) Differential loss of striatal projection neurons in Huntington disease. *Proc. Natl Acad. Sci. USA*, **85**, 5733-5737.
- Wellington, C.L. and Hayden, M.R. (1997) Of molecular interactions, mice and mechanisms: new insights into Huntington's disease. *Curr. Opin. Neurol.*, **10**, 291-298.
- Hackam, A.S., Singaraja, R., Wellington, C.L., Metzler, M., McCutcheon, K., Zhang, T.Q., Kalchman, M. and Hayden, M.R. (1998) The influence of huntingtin protein size on nuclear localization and cellular toxicity. *J. Cell Biol.*, **141**, 1097-1105.
- Ona, V.O., Li, M., Vonsattel, J.P., Andrews, L.J., Khan, S.Q., Chung, W.M., Frey, A.S., Menon, A.S., Li, X.J., Stieg, P.E. *et al.* (1999) Inhibition of caspase-1 slows disease progression in a mouse model of Huntington's disease. *Nature*, **399**, 263-267.
- Chen, M., Ona, V.O., Li, M., Ferrante, R.J., Fink, K.B., Zhu, S., Bian, J., Guo, L., Farrell, L.A., Hersch, S.M. *et al.* (2000) Minocycline inhibits caspase-1 and caspase-3 expression and delays mortality in a transgenic mouse model of Huntington disease. *Nat. Med.*, **6**, 797-801.
- Sanchez, I., Xu, C.J., Joo, P., Kakizaka, A., Blenis, J. and Yuan, J. (1999) Caspase-8 is required for cell death induced by expanded polyglutamine repeats. *Neuron*, **22**, 623-633.
- DiFiglia, M., Sapp, E., Chase, K.O., Davies, S.W., Bates, G.P., Vonsattel, J.P. and Aronin, N. (1997) Aggregation of huntingtin in neuronal intranuclear inclusions and dystrophic neurites in brain. *Science*, **277**, 1990-1993.
- Mende-Mueller, L.M., Toneff, T., Hwang, S.-R., Chesselet, M.-F. and Hook, V.Y.H. (2001) Tissue-specific proteolysis of Huntingtin (htt) in human brain: evidence of enhanced levels of N- and C-terminal htt fragments in Huntington's disease striatum. *J. Neurosci.*, **21**, 1830-1837.
- Kim, Y.J., Yi, Y., Sapp, E., Wang, Y., Cuiffo, B., Kegel, K.B., Qin, Z.-H., Aronin, N. and DiFiglia, M. (2001) Caspase-3-cleaved N-terminal fragments of wild-type and mutant huntingtin are present in normal and

- Huntington's disease brains, associate with membranes, and undergo calpain-dependent proteolysis. *Proc. Natl Acad. Sci. USA*, **98**, 12 784–12 789.
13. Wellington, C.L., Ellerby, L., Gutekunst, C.-A., Rogers, D., Warby, S., Graham, R.K., Loubser, O., Van Raamsdonk, J., Singaraja, R., Yang, Y.-Z. *et al.* (2002) Caspase cleavage of mutant huntingtin precedes neurodegeneration in Huntington disease. *J. Neurosci.*, in press.
 14. Goldberg, Y.P., Nicholson, D.W., Rasper, D.M., Kalchman, M.A., Koide, H.B., Graham, R.K., Bromm, M., Kazemi-Esfarjani, P., Thornberry, N.A., Vaillancourt, J.P. and Hayden, M.R. (1996) Cleavage of huntingtin by apopain, a proapoptotic cysteine protease, is modulated by the polyglutamine tract. *Nat. Genet.*, **13**, 442–449.
 15. Wellington, C.L., Ellerby, L.M., Hackam, A.S., Margolis, R.L., Trifiro, M.A., Singaraja, R., McCutcheon, K., Salvesen, G.S., Propp, S.S., Bromm, M. *et al.* (1998) Caspase cleavage of gene products associated with triplet expansion disorders generates truncated fragments containing the polyglutamine tract. *J. Biol. Chem.*, **273**, 9158–9167.
 16. Wellington, C.L., Singaraja, R., Ellerby, L., Savill, J., Roy, S., Leavitt, B., Cattaneo, E., Hackam, A., Sharp, A., Thornberry, N. *et al.* (2000) Inhibiting caspase cleavage of Huntingtin reduces toxicity and aggregate formation in neuronal and nonneuronal cells. *J. Biol. Chem.*, **275**, 19 831–19 838.
 17. Dyer, R.B. and McMurray, C.T. (2001) Mutant protein in Huntington disease is resistant to proteolysis in affected brain. *Nat. Genet.*, **29**, 270–278.
 18. Martindale, D., Hackam, A., Wiczorek, A., Ellerby, L., Wellington, C., McCutcheon, K., Singaraja, R., Kazemi-Esfarjani, P., Devon, R., Kim, S.U. *et al.* (1998) Length of huntingtin and its polyglutamine tract influences localization and frequency of intracellular aggregates. *Nat. Genet.*, **18**, 150–154.
 19. Mangiarini, L., Sathasivam, K., Seller, M., Cozens, B., Harper, A., Hetherington, C., Lawton, M., Trotter, Y., Leach, H., Davies, S.W. and Bates, G.P. (1996) Exon 1 of the HD gene with an expanded CAG repeat is sufficient to cause a progressive neurological phenotype in transgenic mice. *Cell*, **87**, 493–506.
 20. Menalled, L.B. and Chesselet, M.F. (2002) Mouse models of Huntington's disease. *Trends Pharmacol. Sci.*, **23**, 32–39.
 21. Davies, S.W., Turmaine, M., Cozens, B.A., DiFiglia, L., Sharp, A.H., Ross, C.A., Scherzinger, E., Wanker, E.E., Mangiarini, L. and Bates, G.P. (1997) Formation of neuronal intranuclear inclusions underlies the neurological dysfunction in mice transgenic for the HD mutation. *Cell*, **90**, 537–548.
 22. Hodgson, J.G., Agopyan, N., Gutekunst, C.A., Leavitt, B.R., LePiane, F., Singaraja, R., Smith, D.J., Bissada, N., McCutcheon, K., Nasir, J. *et al.* (1999) A YAC mouse model for Huntington's disease with full-length mutant huntingtin, cytoplasmic toxicity, and selective striatal neurodegeneration. *Neuron*, **23**, 181–192.
 23. Schilling, G., Becher, M.W., Sharp, A.H., Jinnah, H.A., Duan, K., Kotzok, J.A., Slunt, H.H., Ratovitski, T., Cooper, J.K., Jenkins, N.A. *et al.* (1999) Intranuclear inclusions and neuritic aggregates in transgenic mice expressing a mutant N-terminal fragment of huntingtin. *Hum. Mol. Genet.*, **8**, 397–407.
 24. Kim, M., Lee, H.S., LaForet, G., McIntyre, C., Martin, E.J., Chang, P., Kim, T.W., Williams, M., Reddy, P.H., Tagle, D. *et al.* (1999) Mutant huntingtin expression in clonal striatal cells: dissociation of inclusion formation and neuronal survival by caspase inhibition. *J. Neurosci.*, **19**, 964–973.
 25. Li, H., Li, S.-H., Johnston, H., Shelbourne, P.F. and Li, X.-J. (2000) Amino-terminal fragments of mutant huntingtin show selective accumulation in striatal neurons and synaptic toxicity. *Nat. Genet.*, **25**, 385–389.
 26. Boutell, J.M., Thomas, P., Neal, J.W., Weston, V.J., Duce, J., Harper, P.S. and Jones, A.L. (1999) Aberrant interactions of transcriptional repressor proteins with the Huntington's disease gene product, huntingtin. *Hum. Mol. Genet.*, **8**, 1647–1655.
 27. Steffan, J.S., Kazantsev, A., Spasic-Boskovic, O., Greenwald, M., Zhu, Y.Z., Gohler, H., Wanker, E.E., Bates, G.P., Housman, D.E. and Thompson, L.M. (2000) The Huntington's disease protein interacts with p53 and CREB-binding protein and represses transcription. *Proc. Natl Acad. Sci. USA*, **97**, 6763–6768.
 28. Steffan, J.S., Bodai, L., Pallos, J., Poelman, M., McCampbell, A., Apostol, B.L., Kazantsev, A., Schmidt, E., Zhu, Y.Z., Greenwald, M. *et al.* (2001) Histone deacetylase inhibitors arrest polyglutamine-dependent neurodegeneration in *Drosophila*. *Nature*, **413**, 739–743.
 29. Nucifora, F.C., Jr., Sasaki, M., Peters, M.F., Huang, H., Cooper, J.K., Yamada, M., Takahashi, H., Tsuji, S., Troncoso, J., Dawson, V.L. *et al.* (2001) Interference by huntingtin and atrophin-1 with cbp-mediated transcription leading to cellular toxicity. *Science*, **291**, 2423–2428.
 30. Holbert, S., Denghien, I., Kiechle, T., Rosenblatt, A., Wellington, C., Hayden, M.R., Margolis, R.L., Ross, C.A., Dausset, J., Ferrante, R.J. and Neri, C. (2001) The Gln–Ala repeat transcriptional activator CA150 interacts with huntingtin: neuropathologic and genetic evidence for a role in Huntington's disease pathogenesis. *Proc. Natl Acad. Sci. USA*, **98**, 1811–1816.
 31. Kegel, K., Meloni, A.R., Yi, Y., Kim, Y.J., Doyle, E., Cui, B.G., Sapp, E., Wang, Y., Qin, Z.-H., Chen, J.D. *et al.* (2002) Huntingtin is present in the nucleus, interacts with the transcriptional corepressor C-terminal binding protein, and represses transcription. *J. Biol. Chem.*, **277**, 7466–7476.
 32. Dunah, A.W., Jeong, H., Griffin, A., Kim, Y.-M., Standaert, D.G., Hersch, S.M., Mouradian, M.M., Young, A.B., Tanese, N. and Krainc, D. (2002) Sp1 and TAFII130 transcriptional activity disrupted in early Huntington's disease. *Science*, Scienceexpress May 2, 2002.
 33. Li, S.H., Cheng, A.L., Zhou, H., Lam, S., Rao, M., Li, H. and Li, X.J. (2002) Interaction of Huntington disease protein with transcriptional activator Sp1. *Mol. Cell Biol.*, **22**, 1277–1287.
 34. Augood, S.J., Faull, R.L., Love, D.R. and Emson, P.C. (1996) Reduction in enkephalin and substance P messenger RNA in the striatum of early grade Huntington's disease: a detailed cellular in situ hybridization study. *Neuroscience*, **72**, 1023–1036.
 35. Augood, S.J., Faull, R.L.M. and Emson, P.C. (1997) Dopamine D1 and D2 receptor gene expression in the striatum in Huntington's disease. *Ann. Neurol.*, **42**, 215–221.
 36. Andrews, T.C., Weeks, R.A., Turjanski, N., Gunn, R.N., Watkins, L.H., Sahakian, B., Hodges, J.R., Rosser, A.E., Wood, N.W. and Brooks, D.J. (1999) Huntington's disease progression: PET and clinical observations. *Brain*, **122**, 2353–2363.
 37. Cha, J.H., Kosinski, C.M., Kerner, J.A., Alsdorf, S.A., Mangiarini, L., Davies, S.W., Penney, J.B., Bates, G.P. and Young, A.B. (1998) Altered brain neurotransmitter receptors in transgenic mice expressing a portion of an abnormal human huntington disease gene. *Proc. Natl Acad. Sci. USA*, **95**, 6480–6485.
 38. Cha, J.H., Frey, A.S., Alsdorf, S.A., Kerner, J.A., Kosinski, C.M., Mangiarini, L., Penney, J.B., Davies, S.W., Bates, G.P. and Young, A.B. (1999) Altered neurotransmitter receptor expression in transgenic mouse models of Huntington's disease. *Phil. Trans. R. Soc. Lond. B Biol. Sci.*, **354**, 981–989.
 39. Luthi-Carter, R., Strand, A., Peters, N.L., Solano, S.M., Hollingsworth, Z.R., Menon, A.S., Frey, A.S., Spektor, B.S., Penney, E.B., Schilling, G. *et al.* (2000) Decreased expression of striatal signaling genes in a mouse model of Huntington's disease. *Hum. Mol. Genet.*, **9**, 1259–1271.
 40. Li, S.H., Cheng, A.L., Li, H. and Li, X.J. (1999) Cellular defects and altered gene expression in PC12 cells stably expressing mutant huntingtin. *J. Neurosci.*, **19**, 5159–5172.
 41. Wytenbach, A., Swartz, J., Kita, H., Thykjaer, T., Carmichael, J., Bradley, J., Brown, R., Maxwell, M., Schapira, A., Orntoft, T.F. *et al.* (2001) Polyglutamine expansions cause decreased CRE-mediated transcription and early gene expression changes prior to cell death in an inducible cell model of Huntington's disease. *Hum. Mol. Genet.*, **10**, 1829–1845.
 42. Sipione, S., Rigamonti, D., Valenza, M., Zuccato, C., Conti, L., Pritchard, J., Kooperberg, C., Olson, J.M. and Cattaneo, E. (2002) Early transcriptional profiles in huntingtin-inducible striatal cells by microarray analyses. *Hum. Mol. Genet.*, **11**, 1953–1965.
 43. Hughes, R.E., Lo, R.S., Davis, C., Strand, A.D., Neal, C.L., Olson, J.M. and Fields, S. (2001) Altered transcription in yeast expressing expanded polyglutamine. *Proc. Natl Acad. Sci. USA*, **98**, 13 201–13 206.
 44. Luthi-Carter, R., Strand, A.D., Hanson, S.A., Kooperberg, C., Schilling, G., La Spada, M., Merry, D.E., Young, A.B., Ross, C.A., Borchelt, P.R. and Olson, J.M. (2002) Polyglutamine and transcription: gene expression changes shared by DRPLA and Huntington's disease mouse models reveal context independent effects. *Hum. Mol. Genet.*, **11**, 1927–1937.
 45. Laforet, G.A., Sapp, E., Chase, K., McIntyre, C., Boyce, F.M., Campbell, M., Cadigan, B.A., Warzecki, L., Tagle, D.A., Reddy, P.H. *et al.* (2001) Changes in cortical and striatal neurons predict behavioral and electrophysiological abnormalities in a transgenic murine model of Huntington's disease. *J. Neurosci.*, **21**, 9112–9123.
 46. Zuccato, C., Ciammola, A., Rigamonti, D., Leavitt, B.R., Goffredo, D., Conti, L., MacDonald, M.E., Friedlander, R.M., Silani, V., Hayden, M.R.

- et al.* (2001) Loss of huntingtin-mediated BDNF gene transcription in Huntington's disease. *Science*, **293**, 493–498.
47. Cepeda, C., Ariano, M.A., Calvert, C.R., Flores-Hernandez, J., Chandler, S.H., Leavitt, B.R., Hayden, M.R. and Levine, M.S. (2001) NMDA receptor function in mouse models of Huntington disease. *J. Neurosci. Res.*, **66**, 525–539.
 48. Zeron, M.M., Hansson, O., Chen, N., Wellington, C.L., Leavitt, B.R., Brundin, P., Hayden, M.R. and Raymond, L.A. (2002) Increased sensitivity to *N*-methyl-D-aspartate receptor-mediated excitotoxicity in a mouse model of Huntington's disease. *Neuron*, **33**, 1–12.
 49. Luthi-Carter, R., Hanson, S.A., Strand, A.D., Bergstrom, D.A., Chun, W., Peters, N.L., Woods, A.M., Chan, E.Y., Kooperberg, C., Krainc, D. *et al.* (2002) Dysregulation of gene expression in the R6/2 model of polyglutamine disease: parallel changes in muscle and brain. *Hum. Mol. Genet.*, **11**, 1911–1926.
 50. Kiehl, T.-K., Olson, J.M. and Pulst, S.-M. (2001) The Hereditary Disease Array Group (HDAG)—Microarrays, models and mechanisms: a collaboration update. *Curr. Genomics*, **2**, 221–229.
 51. Strand, A.D., Olson, J.M. and Kooperberg, C. (2002) Estimating the statistical significance of gene expression changes observed with oligo-nucleotide arrays. *Hum. Mol. Genet.*, in press.
 52. Schilling, G., Wood, J.D., Duan, K., Slunt, H.H., Gonzales, V., Yamada, M., Cooper, J.K., Margolis, R.L., Jenkins, N.A., Copeland, N.G. *et al.* (1999) Nuclear accumulation of truncated atrophin-1 fragments in a transgenic mouse model of DRPLA. *Neuron*, **24**, 275–286.
 53. Glass, M., Dragunow, M. and Faull, R.L.M. (2000) The pattern of neurodegeneration in Huntington's disease: a comparative study of cannabinoid, dopamine, adenosine and GABA_A receptor alterations in the human basal ganglia in Huntington's disease. *Neuroscience*, **97**, 505–519.
 54. Scherzinger, E., Lurz, R., Turmaine, M., Mangiarini, L., Hollenbach, B., Hasenbank, R., Bates, G.P., Davies, S.W., Lehrach, H. and Wanker, E.E. (1997) Huntingtin-encoded polyglutamine expansions form amyloid-like protein aggregates *in vitro* and *in vivo*. *Cell*, **90**, 549–558.
 55. Leavitt, B.R., Guttman, J.A., Hodgson, J.G., Kimel, G.H., Singaraja, R., Vogl, A.W. and Hayden, M.R. (2001) Wild-type huntingtin reduces the cellular toxicity of mutant huntingtin *in vivo*. *Am. J. Hum. Genet.*, **68**, 313–324.
 56. Rigamonti, D., Bauer, J.H., De-Fraja, C., Conti, L., Sipione, S., Sciorati, C., Clementi, E., Hackam, A., Hayden, M.R., Li, Y. *et al.* (2000) Wild-type huntingtin protects from apoptosis upstream of caspase-3. *J. Neurosci.*, **20**, 3705–3713.